LETTER

doi:10.1038/nature11979

Ovarian surface epithelium at the junction area contains a cancer-prone stem cell niche

Andrea Flesken-Nikitin[1], Chang-Il Hwang[1], Chieh-Yang Cheng[1], Tatyana V. Michurina[2,3], Grigori Enikolopov[2,3] & Alexander Yu. Nikitin[1]

Epithelial ovarian cancer (EOC) is the fifth leading cause of cancer deaths among women in the United States, but its pathogenesis is poorly understood[1–3]. Some epithelial cancers are known to occur in transitional zones between two types of epithelium, whereas others have been shown to originate in epithelial tissue stem cells[4–6]. The stem cell niche of the ovarian surface epithelium (OSE), which is ruptured and regenerates during ovulation, has not yet been defined unequivocally. Here we identify the hilum region of the mouse ovary, the transitional (or junction) area between the OSE, mesothelium and tubal (oviductal) epithelium, as a previously unrecognized stem cell niche of the OSE. We find that cells of the hilum OSE are cycling slowly and express stem and/or progenitor cell markers ALDH1, LGR5, LEF1, CD133 and CK6B. These cells display long-term stem cell properties *ex vivo* and *in vivo*, as shown by our serial sphere generation and long-term lineage-tracing assays. Importantly, the hilum cells show increased transformation potential after inactivation of tumour suppressor genes *Trp53* and *Rb1*, whose pathways are altered frequently in the most aggressive and common type of human EOC, high-grade serous adenocarcinoma[7,8]. Our study supports experimentally the idea that susceptibility of transitional zones to malignant transformation may be explained by the presence of stem cell niches in those areas. Identification of a stem cell niche for the OSE may have important implications for understanding EOC pathogenesis.

An extensive integrated genomic analysis of 489 high-grade serous ovarian adenocarcinomas has provided important insights into the repertoire of molecular aberrations that are characteristic for this most common and deadly form of EOC[7]. However, interpretation of such results is complicated by continuous controversy with regard to the cell of origin of this disease. The OSE, the fimbrial epithelium of the uterine (Fallopian) tubes, and other derivatives of the secondary Mullerian system have been proposed as likely sources of EOC based on pathological observations, genetic and immunohistochemical studies of precursor lesions in human cancer and experimental approaches in several species[2,3,9,10]. Recently, it has been proposed that transitional (or junction) regions between the OSE, mesothelium and tubal epithelium may have more plastic and, presumably, less differentiated states. If this is the case, such regions would be candidate locations of origin of EOC[5,11,12]. However, so far there has been no direct experimental data to support this idea.

Stem cells, such as those of blood and hair, are slow-cycling and retain DNA labels in pulse-chase experiments. OSE cells with some stem and/or progenitor (stem/progenitor) cell properties have been identified previously based on their slow proliferation in label-retention assays[13]. Unfortunately, it remains uncertain whether these cells have potential for long-term self-renewal, a key feature of stem cells. It is also unknown whether these cells occupy anatomically defined areas, similar to those in other organs, such as the intestine, hair follicle, cornea and prostate[14,15]. Activity of the members of the detoxifying enzyme aldehyde dehydrogenase (ALDH) family and the corresponding expression of ALDH1 have been identified as useful markers of stem/progenitor cells in a number of cell lineages, such as mammary, prostate, colon, haematopoietic, neural and mesenchymal cell lineages[16–19]. It has been also reported that approximately 7.6% of OSE cells have high ALDH activity[20]. We therefore tested whether detection of this activity can be used to enrich normal OSE stem/progenitor cells. We separated primary OSE cells into populations with high ALDH expression ($ALDH^+$) and those with low ALDH expression ($ALDH^-$), according to their level of ALDEFLUOR fluorescence by fluorescence-activated cell sorting (FACS, Supplementary Fig. 1), and subjected them to newly established monoclonal OSE-sphere formation assays (Fig. 1a, b and Supplementary Figs 2 and 3). $ALDH^+$ cells represented 5.3% of the OSE population, and they formed larger OSE spheres and at significantly higher frequency compared to $ALDH^-$ cells (Supplementary Fig. 4 and Supplementary Table 1). Consistent with expected self-renewal properties of stem/progenitor cells, spheres were formed from a single-cell suspension in at least five consecutive rounds of sphere dissociation and regeneration (Fig. 1c).

To identify $ALDH1^+$ OSE cells in the mouse ovary we carried out immunohistochemical staining for ALDH1 expression in ovarian tissues from 3-, 6- and 8-week-old virgin FVB/N, C57BL/6J, B6;129 and Swiss Webster mice. As the ovary has well-defined anatomical regions, we evaluated the expression of ALDH1 in the OSE covering the corpus luteum, the distal, antral and the hilum regions, as well as in the tubal epithelium. Notably, in mice of all age and strain groups, cells with high ALDH1 activity were detected predominantly in the hilum region (Fig. 1d and Supplementary Fig. 5). This region represents the point at which nerves and vessels enter the ovary and is covered by the epithelium representing the transition between OSE, mesothelium and tubal epithelium.

To determine the location of slow proliferating cells we carried out pulse-chase experiments by injecting 6- to 7-week-old virgin FVB/N mice for 10 days with a BrdU (5-bromodeoxyuridine) solution, after which we carried out detection of label-retaining cells (LRCs) immediately and monthly for up to 3 months after the pulse (Supplementary Fig. 6a). Ovarian regional analysis has revealed that the hilum contains the highest percentage of slow-cycling OSE cells by 3 months after the BrdU pulse (Fig. 1e and Supplementary Fig. 6b). These LRCs expressed ALDH1, as shown by double immunofluorescence (Fig. 1f). In agreement with earlier reports[13,21], proliferation of OSE was significantly greater after ovulation. To test whether LRCs preferentially divide after ovulation, cells that were double-positive for BrdU and Ki67 were scored in the hilum areas of mice that had been subjected to 2 and 3 months of BrdU pulse-chase experiments and that were euthanized in pro-oestrus (before ovulation) or in oestrus (after ovulation). Double-positive cells were present in the hilum OSE of mice in oestrus only, no such cells were found in pro-oestrus mice (Supplementary Fig. 7), suggesting that these LRCs were activated to repair the ruptured OSE.

We assessed the growth potential of OSE cells isolated by microdissection from the hilum (posterior) and opposite (anterior) regions

[1]Department of Biomedical Sciences and Cornell Stem Cell Program, Cornell University, Ithaca, New York 14853, USA. [2]Cold Spring Harbor Laboratory, Cold Spring Harbor, New York 11724, USA. [3]NBIC, Moscow Institute of Physics and Technology, 123182 Moscow, Russia.

©2013 Macmillan Publishers Limited. All rights reserved

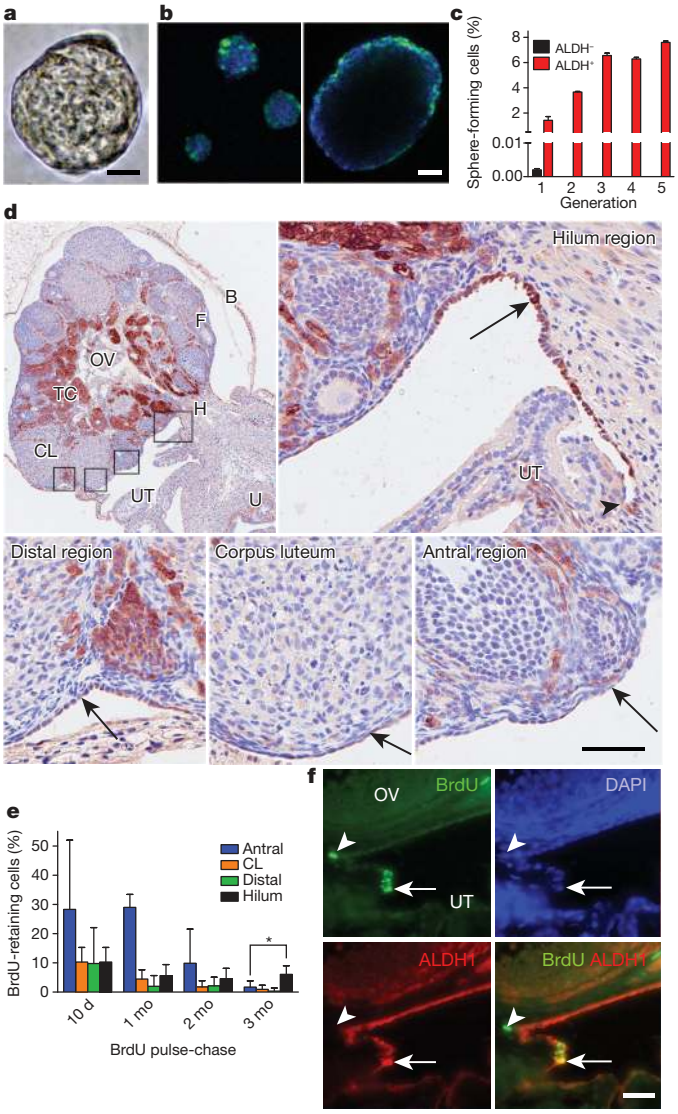

Figure 1 | Identification and location of putative OSE stem cells. **a**, OSE sphere, phase contrast. Scale bar, 20 μm. **b**, Confocal imaging of compact (left) and expanded (right) OSE spheres from *ß-actin-eGFP* mice at 4 and 10 days after placing in culture, respectively. Green fluorescence counterstaining with DAPI (4′,6-diamidino-2-phenylindole), blue. Scale bar, 50 μm. **c**, Frequency of sphere formation by ALDH$^-$ and ALDH$^+$ OSE cells for five consecutive generations (G, dissociation and clonal formation; $n = 6$). ALDH$^-$-derived cells very rarely formed spheres in G2 and did not yield any spheres in G3. **d**, Tissue sections from an ovary of a 6-week-old mouse, stained for ALDH1 expression. ALDH1 (brown) is expressed preferentially in the OSE (arrows) of the hilum region (H) as compared to that of the antral region, corpus luteum (CL) or distal region. ALDH1 staining is also present in the theca cells (TC) of the ovary (OV). Rectangles in the top-left image indicate respective locations (clockwise) of the regions in the mouse ovary. The junction between OSE and tubal epithelium is indicated by an arrowhead. B, bursa; F, follicle; U, uterus; UT, uterine tube. Elite ABC method, haematoxylin counterstaining. Scale bar represents 500 μm (top-left image) or 50 μm (all other images). **e**, Quantification of BrdU label-retaining cells (LRCs) in the antral, corpus luteum (CL), distal and hilum regions ($n = 4$). At 3 months (mo) after BrdU pulse, the percentage of BrdU-retaining cells was significantly higher in the hilum versus antral region (*$P = 0.0005$, two-tailed unpaired *t*-test), versus corpus luteum or distal region ($P < 0.0001$, two-tailed unpaired *t*-test). **f**, Detection of BrdU LRCs (green), ALDH1 (red) and overlay (orange) in the hilum OSE (arrows) after 3 months of chase. Arrowhead, BrdU LRC in the neighbouring stroma. Counterstaining with DAPI, blue. Scale bar, 50 μm. All error bars denote s.d.

of the ovary (Supplementary Fig. 8). After 3 days of primary culture, hilum OSE cells formed significantly more large colonies (≥20 cells) than OSE cells from the anterior region (Fig. 2a, b). Notably, compared to other OSE cells, hilum cells developed spheres at significantly higher frequency and could be propagated for at least 7 generations (Fig. 2c, Supplementary Fig. 9 and Supplementary Table 2). These findings are consistent with results of our previous experiments with ALDH$^+$ cells.

For additional phenotypical characterization, ALDH$^+$ and ALDH$^-$ OSE cells were isolated by FACS and their RNA used for gene-expression profiling (Fig. 2d, Supplementary Fig. 10 and Supplementary Table 3). *Aldh1* gene was among the most highly expressed genes in ALDH$^+$ cells (Supplementary Fig. 10). LGR5, CD133 (also known as prominin 1), CK6B and LEF1 were consistently more highly expressed than other known stem cell markers in ALDH$^+$ cells (Fig. 2e). Expression of these markers in the hilum cells was also confirmed by immunostaining (Fig. 2f). Consistent with this, we have found that some of the

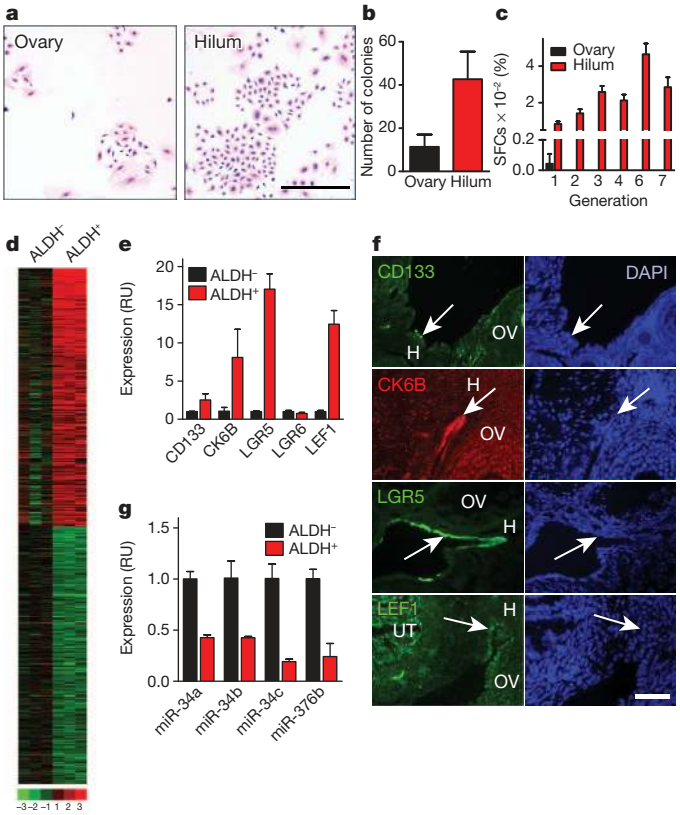

Figure 2 | Functional characterization of the hilum OSE cells. **a**, Colony formation by OSE cells isolated from the anterior region of the ovary and the hilum, shown by Giemsa staining. 1×10^4 cells were cultured per plate. Scale bar, 500 μm. **b**, Quantitative analysis of the frequency of large colonies (≥20 cells) formed by OSE cells from the anterior part ($n = 8$) and the hilum ($n = 6$). $P < 0.0001$, two-tailed unpaired *t*-test. **c**, Frequency of OSE sphere-forming cells (SFCs) in the anterior region of the ovary and hilum for seven consecutive generations (G, $n = 3$). Cells derived from the anterior region of the ovary very rarely formed spheres in G2 and did not produce any spheres in G3. **d**, Gene-expression profiles of 3 independent pools ($n = 10$ mice each) of ALDH$^-$ and ALDH$^+$ cells. The keys shows fluorescence expression ratios ($\log_2$ transformed). **e**, Expression of stem cell markers in ALDH$^-$ and ALDH$^+$ cells. Quantitative real-time polymerase chain reaction (rtPCR) ($n = 3$, $P < 0.01$ in all cases, except for LGR6). RU, relative units. **f**, Detection of hilum cells (arrows) expressing CD133, CK6B, LGR5 and LEF1. Immunofluorescence (CD133, CK6B, and LEF1) or eGFP expression under the control of the *Lgr5* promoter in *Lgr5-eGFP-IRES-CreERT2* mice. Counterstaining with DAPI, blue. Scale bar, 50 μm. **g**, Expression of microRNAs in ALDH$^-$ and ALDH$^+$ cells. Quantitative rtPCR ($n = 3$, $P < 0.01$ in all cases). All error bars denote s.d.

©2013 Macmillan Publishers Limited. All rights reserved

microRNAs that counteract stem cell properties, such as microRNAs of the miR-34 family[22–24], and miR-376b (Palmaccio, S. J., Cheng, L., A.F.-N. and A.Yu.N., unpublished observations), are preferentially downregulated in ALDH$^+$ OSE cells relative to the ALDH$^-$ OSE population (Fig. 2g).

As hilum cells express LGR5, to trace the fate of these cells we used *Lgr5*$^{tm1(cre/ERT2)Cle}$*/J* mice, which harbour an *Lgr5-eGFP-IRES-CreERT2* knock-in allele[25]. In these mice, enhanced green fluorescent protein (eGFP) and Cre–ERT2 are expressed in LGR5-positive cells. However, activity of Cre–ERT2 fusion protein occurs only after induction by tamoxifen. We crossed *Lgr5*$^{tm1(cre/ERT2)Cle}$*/J* mice with *Gt(ROSA)26Sor*$^{tm9(CAG\text{-}tdTomato)Hze}$*/J* (Ai9) mice (Supplementary Fig. 11). In Ai9 mice, expression of red fluorescent protein variant (tdTomato) under the control of *CAG* promoter at the *Rosa26* locus is possible only after Cre-mediated deletion of the stop codon flanked by *loxP* sites[26]. To test whether *Lgr5* promoter directs Cre expression to the hilum cells, mice were exposed to a single dose of tamoxifen and their ovaries were collected 1 and 3 days later. Microscopy analysis showed that cells of the hilum were exclusively labelled in the OSE at these early time points (Fig. 3a–c and Supplementary Fig. 12a–g). Control experiments included administration of oil to double-knock-in littermates (Fig. 3d, e and Supplementary Fig. 12h–j). Furthermore, wild-type mice and mice carrying only one of the knock-in alleles were analysed with and without tamoxifen administration. To test whether LGR5-expressing hilum cells contribute to the rest of the OSE, we collected ovaries of *Lgr5-eGFP-IRES-CreERT2* Ai9 mice, 1 and 2 months after tamoxifen administration. The majority of OSE cells in tamoxifen but not control experiments expressed tdTomato, indicating that the hilum cells contribute to regeneration of the OSE covering the ovary (Fig. 3f and Supplementary Fig. 12k, l).

Trp53 (transformation-related protein 53) mutations and alterations of the RB1 (retinoblastoma 1) pathway occur in 96% and 67% of human high-grade serous adenocarcinomas, respectively[7,8], and result in formation of similar malignancies in genetically modified mice[27,28]. We therefore compared proliferation and immortalization efficiency of the OSE cells located at the hilum and in the remainder of the ovary after conditional inactivation of *Trp53* and *Rb1* (Supplementary Fig. 13). The hilum cells showed significantly increased proliferation and were passaged over 20 times without reaching crisis phase. In contrast, the majority of the remaining OSE cell pool became senescent by passage 6, according to their enlarged flattened shape and expression of senescence markers, such as senescence-associated β-galactosidase, p16 and p27 (Fig. 4a–c and Supplementary Fig. 14).

We evaluated various regions of the ovary carefully for the early stages of carcinogenesis induced by Cre-*loxP*-mediated recombination after a single administration of adenovirus expressing Cre (AdCre) into the ovarian bursa. Such administration results in infection of more than 80% of cells in all anatomical regions of the ovary and then formation of *Trp53*- and *Rb1*-deficient neoplastic lesions in a relatively synchronous manner (Supplementary Figs 15, 16 and ref. 27). The earliest atypical cells were detected in the hilum and adjacent areas but not in the other regions of the ovary or in the tubal epithelium in 12 out of 16 mice (75%) by 60 days after induction (Supplementary Fig. 17 and Supplementary Table 4).

To test the tumorigenic properties of *Trp53*- and *Rb1*-deficient primary OSE cells, we transplanted them intraperitoneally and subcutaneously. In intraperitoneal experiments, seven out of eight mice (87%) that were transplanted with the hilum cells developed high-grade serous adenocarcinomas characterized by extensive proliferation and expression of cytokeratin 8 (CK8), Wilms tumour protein (WT1), PAX8, oestrogen receptor 1 (ER), ephrin B1 and ALDH1 (Fig. 4d–n and Supplementary Figs 18 and 19). Notably, 5 out of 7 neoplasms (71%) metastasized to the lung (Fig. 4l–n and Supplementary Fig. 18d–f). Only 1 out of 12 mice (8%) that were transplanted with the remaining OSE cells developed carcinoma. This neoplasm expressed CK8, WT1 and ER, but contained less cells with high

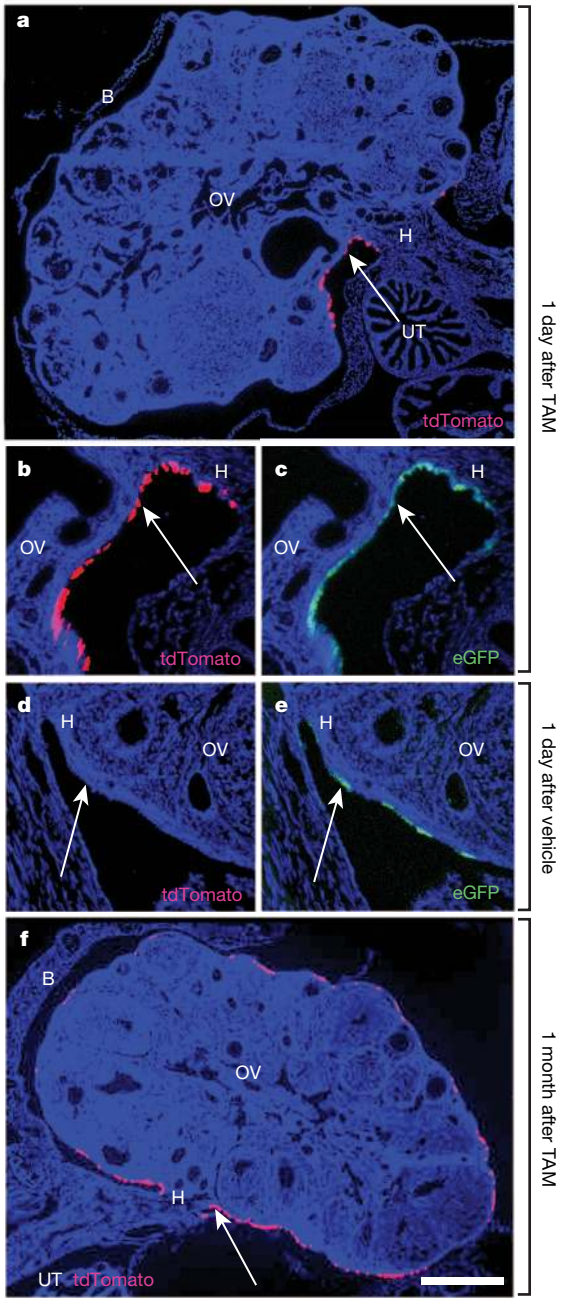

Figure 3 | Tracing the fate of LGR5$^+$ hilum cells. a–f, Detection of tdTomato (red; **a**, **b**, **d** and **f**) and eGFP (green; **c** and **e**) expression in the ovaries of *Lgr5-eGFP-IRES-CreERT2* Ai9 mice, 1 day (**a**–**e**) and 1 month (**f**) after administration of either tamoxifen (TAM; **a**–**c** and **f**) or vehicle (**d** and **e**). Counterstaining with DAPI, blue. Arrows, hilum OSE. Scale bar represents 600 μm (**a** and **f**) or 130 μm (**b**–**e**).

ALDH1 expression and only a few PAX8-positive cells, and it was not metastatic (Supplementary Figs 19 and 20). Similar results were also observed in subcutaneous experiments (Supplementary Figs 19–21 and Supplementary Table 5). Thus, the hilum cells have increased transformation potential after inactivation of *Trp53* and *Rb1* and may be the cell of origin of EOC.

In summary, we show that the OSE at junction areas contains a novel stem cell niche that is responsible for OSE regeneration and is prone to malignant transformation. These findings provide experimental rationale for targeted detection and characterization of pre-neoplastic and early neoplastic lesions in the areas of transition between OSE, mesothelium and tubal epithelium in humans. Previously, presence of

©2013 Macmillan Publishers Limited. All rights reserved

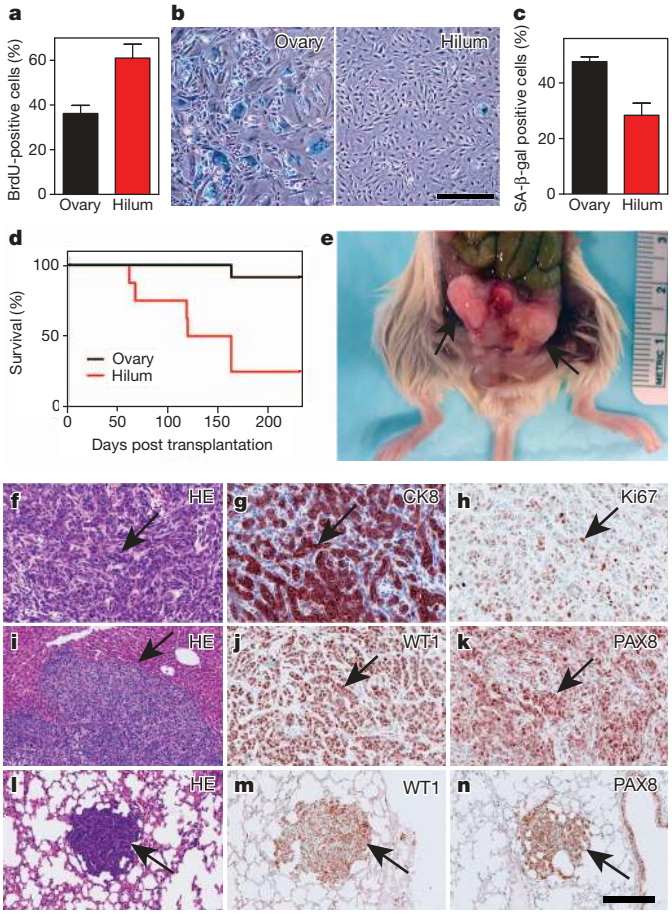

Figure 4 | Hilum cells show preferential transformation after conditional inactivation of *Trp53* and *Rb1*. Characterization of primary OSE cells isolated from the hilum and the remainder of the ovary, and evaluated at passage 6 after Cre-*loxP*-mediated inactivation of *Trp53* and *Rb1*. **a**, Quantification of BrdU-positive OSE cells ($n = 3$, $P < 0.0001$, two-tailed unpaired *t*-test). **b**, **c**, Detection (**b**) and quantitative analysis (**c**) of senescence-associated β-galactosidase (SA-β-gal; blue) in the ovary and hilum cells ($n = 3$, $P = 0.002$, two-tailed unpaired *t*-test), using phase contrast microscopy. Scale bar in **b**, 500 μm. **d**, Survival of mice that were intraperitoneally transplanted with primary ovary ($n = 12$) and hilum ($n = 8$) OSE cells deficient for *Trp53* and *Rb1* (log-rank $P = 0.0007$). **e**, Neoplastic masses (arrows) from hilum cells transplanted into the mouse abdominal cavity. **f**–**n**, Hilum-derived neoplastic cells have marked nuclear atypia (**f**), express cytokeratin 8 (CK8, **g**), are highly proliferative (**h**), grow in solid, nested and gland-like patterns (**f**–**h**, **j** and **k**, arrows), invade liver (**i**, arrow), metastasize to the lung (**l**–**n**, arrows) and express Wilms tumour protein (WT1; **j** and **m**) and PAX8 (**k** and **n**). Haematoxylin and eosin (HE) and immunostaining, Elite ABC method. Counterstaining with haematoxylin (CK8) and methyl green (Ki67, WT1 and PAX8). Scale bar represents 100 μm (**f**–**h**, **j** and **k**) or 200 μm (**i** and **l**–**n**). All error bars denote s.d.

adult stem cells in the areas of a junction between two types of epithelia was demonstrated definitively for the limbus region, a narrow transitional zone between the cornea and bulbar conjunctiva[29], and for the gastroesophageal junction[30]. However, it remains unclear whether such junction-associated stem cell niches are predisposed to cancer. Our findings support this possibility and suggest that similar junction areas in other organs, such as the uterine cervix and the anus, may also contain cancer-prone stem cell niches, thereby explaining susceptibility of such regions to malignant transformation. Given the anatomically well-defined location of the hilum in the mouse ovary, this region may represent an attractive model for further studies aimed at understanding why stem cell niches reside in the junction areas and how aberrations in the molecular and cellular mechanisms governing epithelium regeneration may contribute to ovarian carcinoma pathogenesis.

METHODS SUMMARY

Primary antibodies used for immunohistochemistry are listed in Supplementary Table 6. Cell culture, molecular, histology and pathology techniques, as well as carcinogenesis experiments, were carried out as described previously[27] and in the Methods section.

Full Methods and any associated references are available in the online version of the paper.

Received 19 January 2012; accepted 1 February 2013.
Published online 6 March 2013.

1. Siegel, R., Naishadham, D. & Jemal, A. Cancer statistics, 2012. *CA Cancer J. Clin.* **62,** 10–29 (2012).
2. Lengyel, E. Ovarian cancer development and metastasis. *Am. J. Pathol.* **177,** 1053–1064 (2010).
3. Bowtell, D. D. The genesis and evolution of high-grade serous ovarian cancer. *Nature Rev. Cancer* **10,** 803–808 (2010).
4. Visvader, J. E. Cells of origin in cancer. *Nature* **469,** 314–322 (2011).
5. Auersperg, N. The origin of ovarian carcinomas: a unifying hypothesis. *Int. J. Gynecol. Pathol.* **30,** 12–21 (2011).
6. Medema, J. P. & Vermeulen, L. Microenvironmental regulation of stem cells in intestinal homeostasis and cancer. *Nature* **474,** 318–326 (2011).
7. The Cancer Genome Atlas Research Network. Integrated genomic analyses of ovarian carcinoma. *Nature* **474,** 609–615 (2011).
8. Ahmed, A. A. *et al.* Driver mutations in *TP53* are ubiquitous in high grade serous carcinoma of the ovary. *J. Pathol.* **221,** 49–56 (2010).
9. Kurman, R. J. & Shih Ie, M. The origin and pathogenesis of epithelial ovarian cancer: a proposed unifying theory. *Am. J. Surg. Pathol.* **34,** 433–443 (2010).
10. Dubeau, L. The cell of origin of ovarian epithelial tumours. *Lancet Oncol.* **9,** 1191–1197 (2008).
11. Auersperg, N., Woo, M. M. & Gilks, C. B. The origin of ovarian carcinomas: a developmental view. *Gynecol. Oncol.* **110,** 452–454 (2008).
12. Seidman, J. D., Yemelyanova, A., Zaino, R. J. & Kurman, R. J. The fallopian tube-peritoneal junction: a potential site of carcinogenesis. *Int. J. Gynecol. Pathol.* **30,** 4–11 (2011).
13. Szotek, P. P. *et al.* Normal ovarian surface epithelial label-retaining cells exhibit stem/progenitor cell characteristics. *Proc. Natl Acad. Sci. USA* **105,** 12469–12473 (2008).
14. Blanpain, C., Horsley, V. & Fuchs, E. Epithelial stem cells: turning over new leaves. *Cell* **128,** 445–458 (2007).
15. Simons, B. D. & Clevers, H. Strategies for homeostatic stem cell self-renewal in adult tissues. *Cell* **145,** 851–862 (2011).
16. Ginestier, C. *et al.* ALDH1 is a marker of normal and malignant human mammary stem cells and a predictor of poor clinical outcome. *Cell Stem Cell* **1,** 555–567 (2007).
17. Storms, R. W. *et al.* Isolation of primitive human hematopoietic progenitors on the basis of aldehyde dehydrogenase activity. *Proc. Natl Acad. Sci. USA* **96,** 9118–9123 (1999).
18. Corti, S. *et al.* Identification of a primitive brain-derived neural stem cell population based on aldehyde dehydrogenase activity. *Stem Cells* **24,** 975–985 (2006).
19. Burger, P. E. *et al.* High aldehyde dehydrogenase activity: a novel functional marker of murine prostate stem/progenitor cells. *Stem Cells* **27,** 2220–2228 (2009).
20. Deng, S. *et al.* Distinct expression levels and patterns of stem cell marker, aldehyde dehydrogenase isoform 1 (ALDH1), in human epithelial cancers. *PLoS ONE* **5,** e10277 (2010).
21. Bullough, W. S. Oogenesis and its relation to the oestrous cycle in the adult mouse. *J. Endocrinol.* **3,** 141–149 (1942).
22. Ji, Q. *et al.* MicroRNA miR-34 inhibits human pancreatic cancer tumor-initiating cells. *PLoS ONE* **4,** e6816 (2009).
23. Liu, C. *et al.* The microRNA miR-34a inhibits prostate cancer stem cells and metastasis by directly repressing CD44. *Nature Med.* **17,** 211–215 (2011).
24. Choi, Y. J. *et al.* miR-34 miRNAs provide a barrier for somatic cell reprogramming. *Nature Cell Biol.* **13,** 1353–1360 (2011).
25. Barker, N. *et al.* Identification of stem cells in small intestine and colon by marker gene *Lgr5*. *Nature* **449,** 1003–1007 (2007).
26. Madisen, L. *et al.* A robust and high-throughput Cre reporting and characterization system for the whole mouse brain. *Nature Neurosci.* **13,** 133–140 (2010).
27. Flesken-Nikitin, A., Choi, K. C., Eng, J. P., Shmidt, E. N. & Nikitin, A. Y. Induction of carcinogenesis by concurrent inactivation of *p53* and *Rb1* in the mouse ovarian surface epithelium. *Cancer Res.* **63,** 3459–3463 (2003).
28. Szabova, L. *et al.* Perturbation of Rb, p53, and Brca1 or Brca2 cooperate in inducing metastatic serous epithelial ovarian cancer. *Cancer Res.* **72,** 4141–4153 (2012).
29. Pellegrini, G. *et al.* Location and clonal analysis of stem cells and their differentiated progeny in the human ocular surface. *J. Cell Biol.* **145,** 769–782 (1999).
30. Barker, N. *et al.* Lgr5^{+ve} stem cells drive self-renewal in the stomach and build long-lived gastric units *in vitro*. *Cell Stem Cell* **6,** 25–36 (2010).

Supplementary Information is available in the online version of the paper.

Acknowledgements We would like to thank T. Tumbar for critical reading of this manuscript, J. Choi for help with immunostainings, L. Sayam (NYSTEM supported FACS Core) for help with FACS experiments and F. M. Vermeylen (Cornell Statistical Consulting Unit) for help with statistical analysis. This work was supported by grants

©2013 Macmillan Publishers Limited. All rights reserved

from the US National Institutes of Health (NIH) and National Cancer Institute (NCI) (CA096823 and CA112354), NYSTEM (C023050 and N11G-160) and the Marsha Rivkin Center for Ovarian Cancer Research to A.Yu.N.; the NIH National Institute of Mental Health (MH092928), NIH National Institute on Aging (AG040209), NYSTEM (C024323) and Russian Ministry of Education and Science to G.E.; and postdoctoral fellowships to A.F.-N. (NIH NICHD T32HD052471) and C-.I.H. (Cornell Comparative Cancer Biology Training Program).

Author Contributions A.F.-N. and A.Yu.N. designed the study, interpreted data and wrote the manuscript. A.F.-N., C.-I.H., C.-Y.C., T.V.M. and G.E. performed experiments and analysed data. All authors discussed the results and commented on the manuscript.

Author Information Microarray data discussed in this publication have been deposited in the National Center for Biotechnology Information (NCBI) Gene Expression Omnibus and are accessible through GEO Series accession number GSE43897. Reprints and permissions information is available at www.nature.com/reprints. The authors declare no competing financial interests. Readers are welcome to comment on the online version of the paper. Correspondence and requests for materials should be addressed to A.Yu.N. (an58@cornell.edu).

©2013 Macmillan Publishers Limited. All rights reserved

METHODS

Experimental animals. FVB/NCr (FVB/N) and Swiss Webster (Cr:SW) mice were obtained from NCI-Frederick Animal Production Program (Charles River Laboratories) or bred in-house. C57BL/6J (B6) mice and B6 × 129 crosses were bred in-house. The C57BL/6-Tg(CAG-eGFP)1Osb/J (*β-actin-eGFP*), B6.Cg-Tg(CAG-DsRed*MST)1Nagy/J (*β-actin-DsRed*), *Lgr5*$^{tm1(cre/ERT2)Cle}$/J (*Lgr5-eGFP-IRES-CreERT2*), *Gt(ROSA)26Sor*$^{tm9(CAG-tdTomato)Hze}$/J (Ai9) and *NOD.Cg-Prkdc*^{scid}*Il2rg*^{tm1Wjl}/*SzJ* mice were obtained from The Jackson Laboratory. *Trp53*$^{loxP/loxP}$ and *Rb1*$^{loxP/loxP}$ mice (*Trp53* and *Rb1* genes carrying floxed alleles) were a gift from A. Berns. All mice were maintained identically, following recommendations of the Institutional Laboratory Animal Use and Care Committee.

Isolation of primary OSE cells. Individual ovaries were dissected from 6- to-8-week-old virgin FVB/N or wild-type mice, transferred to 100 µl digestion buffer (4 mg Collagenase-Dispase (Roche) per ml DMEM/F12 (Ham's) medium (Mediatech) supplemented with 30 mg ml^{-1} bovine albumin (Sigma) and 1 µl DNase I (1 mg ml^{-1}, Sigma)), incubated for 55 min at 37 °C in a 5% CO_2 incubator. After the incubation, ovaries were removed and 5 ml complete OSE stem cell medium (OSE SCM) was added. OSE SCM consists of 5% fetal bovine serum (FBS; Sigma), 4 mM L-glutamine (Mediatech), 1 mM sodium pyruvate (Mediatech), 10 ng ml^{-1} epidermal growth factor (Sigma), 500 ng ml^{-1} hydrocortisone (Sigma), 5 µg ml^{-1} insulin (Sigma), 5 µg ml^{-1} transferrin (Sigma), 5 ng ml^{-1} sodium selenite (Sigma), 0.1 mM MEM non-essential amino acids (Mediatech), 10^{-4} M β-mercaptoethanol (Sigma), 10^3 units per ml leukaemia inhibitory factor (Millipore) in DMEM/F12 (Ham's) medium (Mediatech). Cells were collected by centrifugation, and 2×10^4 cells were seeded onto one gelatinized 24-well plate and incubated in OSE SCM at 5% CO_2 for 24 h to eliminate accidental non-OSE cells[27,31,32]. The purity of isolated cells was confirmed by RT–PCR (PCR with reverse transcription) detection of CK8 expression.

ALDEFLUOR assay and fluorescence-activated cell sorting. For detection of ALDH enzymatic activity, primary OSE cells (4×10^6) were placed in ALDEFLUOR buffer and processed for staining with the ALDEFLUOR kit (Aldagen) according to the manufacturer's protocol. Cell sorting and data analysis were performed on a FACS Aria II sorter equipped with the FACS DiVa software (BD Bioscience). Unstained cells and cells treated with ALDH inhibitor (4-(diethylamino)benzaldehyde[33] at a tenfold molar excess) served as controls. Dead cells were excluded with propidium iodide. The brightest 5–8% of ALDH$^+$ cells were identified and gated electronically based on their characteristic light-scatter properties on the fluorescein isothiocyanate (FITC)-channel emission pattern after excitation with a 13–20 mW, 488-nm ellipse-shaped laser (elliptical) BD FACSAria II. The ALDH fluorescence emissions were captured simultaneously through a 515/20-nm band-pass and 505-nm long-pass filter. ALDH$^+$ and ALDH$^-$ OSE cells were collected in 0.5 ml OSE SCM and subjected to OSE-sphere rim assays or RNA isolation, as described below.

OSE-sphere-formation rim assay. Cell populations (5×10^5 cells per assay) were collected in 0.5 ml OSE SCM and centrifuged, and pellets were suspended in reduced growth-factor basement-membrane matrix (Geltrex, Invitrogen) and OSE SCM (1:1 ratio) in a total volume of 120 µl. A modified protocol of Lawson *et al.*[34] was followed; cells were placed around the rim of a well of a 12-well plate and allowed to solidify for 25 min at 37 °C in a 5% CO_2 incubator before adding 1.5 ml OSE SCM. Spheres were grown for 7 to 12 days. For passaging of spheres, media were aspirated and Geltrex was digested by incubation in 750 µl digestion buffer for 1 h, at 37 °C. During incubation, spheres were suspended 2 to 3 times manually by pipetting through a blue 1-ml pipette tip. Digested cultures were pelleted and incubated in 0.3 ml 0.25% trypsin/EDTA for 10 min at 37 °C, cells were suspended and the enzyme reaction was stopped by adding 4 ml OSE SCM. Cells were collected and counted using a haemocytometer, and then cultured at different densities.

Confocal imaging of OSE-sphere suspension culture. Primary OSE cells from *β-actin-eGFP* mice were grown for 4 or 10 days in low-attachment 24-wells (Corning) at 2×10^4 cells per ml OSE stem cell conditioned medium, which was composed of the following: (DMEM/F12 (Ham's) medium (Mediatech) containing 2.4% methylcellulose (Sigma), 0.4% BSA (Sigma), 4 mM L-glutamine (Mediatech), 1 mM sodium pyruvate (Mediatech), 10 ng ml^{-1} epidermal growth factor (Sigma), 500 ng ml^{-1} hydrocortisone (Sigma), 5 µg ml^{-1} insulin (Sigma), 5 µg ml^{-1} transferrin (Sigma), 5 ng ml^{-1} sodium selenite (Sigma), 10 ng ml^{-1} fibroblast growth factor basic (Sigma), 0.1 mM MEM non-essential amino acids (Mediatech), 10^3 units per ml leukaemia inhibitory factor (Millipore), 10^{-4} M β-mercaptoethanol (Sigma). Using a drawn-out glass capillary under a dissection microscope, spheres were washed twice for 3 min in a drop of PBS at room temperature (20–22 °C), fixed in 4% paraformaldehyde for 5 min, washed twice with PBS, once with ddH_2O, stained with DAPI (Sigma, 1 mg ml^{-1}) for 5 min, transferred to a glass slide, mounted in Fluorogel (Electron Microscopy Sciences) and covered by a glass coverslip. Confocal pictures were acquired at room temperature using a Zeiss LSM 510 Meta confocal microscope coupled with an Axiovert 200 inverted microscope (Carl Zeiss). Optical sections, 512 × 512 pixels, were collected sequentially for each fluorochrome. The data sets acquired were merged and displayed with the ZEN software (Zeiss).

Monoclonality assays. Two approaches were used. First, similarly to earlier studies in other cell types[34–36], single-cell suspensions of primary OSE cells from *β-actin-eGFP* or *β-actin-DsRed* mice were mixed at various ratios, grown in OSE-sphere-forming rim assays for 7–12 days without subculture in stem cell conditioned medium, and then the numbers of monochromatic and dichromatic spheres were counted. Second, the development of spheres from individual cells in rim assays was monitored by imaging the same fields of view at different time points. All images were collected using a Nikon Eclipse TS100 microscope coupled with an Epi-Fluorescence Attachment (Nikon), equipped with a DS-L2 camera control unit and cooled camera head DS-5Mc (Nikon).

Primary culture of regions of the hilum and ovary. Individual hilum and anterior ovary regions were isolated under dissection microscope from adult virgin FVB/N mice, minced in a drop of PBS with 25G needles and transferred to 100 µl of digestion buffer. Samples were then incubated as described for the isolation of primary OSE cells. After 24 h, adherent cultures of cells from the hilum and anterior ovary region were collected and seeded out for the cell proliferation or OSE-sphere rim assays.

Gene-expression arrays. Total RNA was isolated using a mirVana miRNA isolation kit (Ambion). An Ovation Pico WTA System V2 (NuGen) was used to amplify complementary DNA, and this was then labelled with biotin using Encore Biotin Module (NuGen). Labelled DNA was hybridized onto an Affymetrix Mouse Genome 430 2.0 array (Affymetrix). All microarray analyses were carried out as described previously[31,32,37,38]. In briefly, microarray data were analysed with GeneSifter software (Geospiza). To identify genes that were significantly altered in ALDH-positive populations, we carried out paired two-group analysis using Significance Analysis of Microarrays (SAM) software (http://www-stat.stanford.edu/~tibs/SAM/) and visualizations using Treeview software (http://rana.lbl.gov).

***Trp53* and *Rb1* inactivation in primary OSE cells.** Individual samples of hilum regions, and all ovary regions except the hilum, were isolated under a dissection microscope from adult *Trp53*$^{loxP/loxP}$*Rb1*$^{loxP/loxP}$ mice, and then incubated as described for the isolation of primary OSE cells. Cells were passaged one or two times and treated with recombinant adenoviruses essentially as described previously[27,31]. No changes in composition of ALDH1$^+$- and ALDH$^-$-cell subpopulations were observed between cells tested 24 h after initial adherent culture and cells tested immediately before exposure to adenovirus. At passage 6 after *Trp53* and *Rb1* inactivation, proliferation- and senescence-detection assays were carried out as described below.

Cell-proliferation assays. Primary cells from the hilum and ovary regions, passage 0, were collected, reseeded in triplicate at 1×10^4 cells per 3.5-cm dish in OSE SCM, grown for 3 days, then stained with Giemsa solution (Sigma), air-dried and analysed in a total area of 4.92 cm^2. For BrdU staining, cells were incubated with 3 µg ml^{-1} BrdU for 2 h at 37 °C and fixed with 4% paraformaldehyde. DNA was denatured using 4N HCl with 0.5% Triton X-100 (Sigma) at room temperature for 10 min, and cells were washed in Tris-buffered saline with 0.5% Triton X-100. Primary antibody for BrdU (Supplementary Table 6) was applied overnight at 4 °C, and cells were then incubated with secondary biotinylated antibody (1 h at room temperature) and a modified avidin–biotin–peroxidase technique was used as described previously[39].

Senescence-detection assays. For detection of senescence-associated β-galactosidase, OSE cells were fixed with 2% formaldehyde/0.2% glutaraldehyde for 5 min, rinsed several times with PBS, and incubated in senescence-associated β-galactosidase staining solution (4.2 mM citric acid, 12.5 mM sodium phosphate, 158 mM sodium chloride, 0.21 mM magnesium chloride, 2.21 mg ml^{-1} potassium ferrocyanide, 1.68 mg ml^{-1} potassium ferricyanid (all Sigma), 1 mg ml^{-1} 5-bromo-4-chloro-3-indolyl β-D-galoctosidase (X-Gal, Invitrogen), pH 6.0) for 24 h at 37 °C according to a published protocol[40]. For immunofluorescent detection of p16 and p27, cells were fixed with 4% paraformaldehyde and incubated with primary antibodies (Supplementary Table 6) overnight at 4 °C. Secondary antibody (Alexa Fluor 488 conjugate, Invitrogen) was applied for 1 h at room temperature. DAPI was used for nuclear counterstaining.

BrdU pulse-chase experiments. Six- to seven-week-old virgin FVB/N mice were injected daily with 250 µl of BrdU (Sigma; 1 mg ml^{-1}) intraperitoneally for 10 days (pulse) and euthanized immediately after the pulse, or 1, 2 or 3 months after pulse, in 3 independent experiments. For LCR-proliferation analysis during the oestrus cycle, the stage of the oestrus cycle was checked by vaginal cytology and mice were euthanized either during pro-oestrus (before ovulation) or oestrus (after ovulation), after 2 or 3 months of chase.

©2013 Macmillan Publishers Limited. All rights reserved

Cell-lineage tracing. To deliver the tamoxifen pulse, 6- to 7-week-old virgin *Lgr5-eGFP-IRES-CreERT2* Ai9 and control mice were injected intraperitoneally with a single dose of tamoxifen (Sigma, 0.2 mg g^{-1} body weight, 25 mg ml^{-1} in corn oil) or three doses every other day for 6 days. Ovaries of tamoxifen-pulsed mice were collected 1 and 3 days after the pulse, and at monthly intervals for 2 months. Collected ovaries were fixed with 4% paraformaldehyde for 2 h at room temperature, washed twice for 3 min with PBS, kept overnight at 4 °C, embedded in Tissue-Tek OCT compound (Sakura Fineted) and frozen in liquid nitrogen. Frozen sections were counterstained with DAPI (Sigma, 1 mg ml^{-1}) and images were taken with an Axioskop 2 fluorescence microscope (Zeiss) equipped with a charge-coupled device (CCD) camera.

Intrabursal administration of adenovirus and carcinogenesis induction. At oestrus, adult *Trp53*$^{loxP/loxP}$*Rb1*$^{loxP/loxP}$ mice received a single trans-infundibular intrabursal injection of recombinant adenovirus AdCre-eGFP, AdCre, AdeGFP or AdBlank (Gene Transfer Vector Core) as described previously[27]. The original stock solution (stored at −80 °C) with a titre of 7×10^{10} plaque-forming units per ml was diluted at a ratio of 1:20 with PBS at room temperature immediately before the injection.

Laser microdissection and PCR genotyping. For microdissection of frozen sections, 5-μm-thick frozen sections of the mouse ovaries were placed on slides for membrane-based laser microdissection (Leica Microsystems) and evaluated under the Leica DM LA microscope coupled with a Fluorescence illuminator LRF 4/22. eGFP-expressing OSE from the hilum and different ovarian regions were microdissected using the Leica AS LMD laser-microdissection system (Leica) equipped with a VSL-337ND-S nitrogen laser. Phase-contrast and fluorescent images were acquired before and after the microdissection. Manual microdissection of haematoxylin-and-eosin-stained sections was carried out essentially as described preciously[27,39,41]. Tissues were collected into caps of 0.6-ml centrifuge tubes filled with lysis buffer and used for subsequent PCR amplification prepared as described previously[27,37,39,42,43].

Tumorigenicity assays. Primary OSE cells deficient for *Trp53* and *Rb1* were derived from primary hilum, or all ovary regions except the hilum, and were suspended in PBS and injected intraperitoneally (8×10^6 cells in 500 μl) or subcutaneously ($5 \times 10^4 - 5 \times 10^6$ cells in 250 μl) into 5-week-old *NOD.Cg-Prkdc*^{scid}*Il2rg*^{tm1Wjl}/*SzJ4* female mice. As soon as signs of sickness were seen (for example, abdominal distention, intra-abdominal masses or subcutaneous masses over 1 cm in diameter or moribund behaviour), mice were euthanized and subjected to necropsy.

Morphological evaluation. Owing to the coiled structure of the mouse uterine tubes[44], 4-μm-thick paraffin serial sections within 100 μm of the junction between the OSE and tubal epithelium were used for all studies of the hilum region. Serial sections were also evaluated to exclude potential misinterpretation of tangential sections in all relevant quantitative assays. All mice in carcinogenesis experiments were subjected to gross pathology evaluation during necropsy. Particular attention was paid to potential sites of ovarian carcinoma spreading, such as the omentum, regional lymph nodes, liver, lung and mesentery. In addition to the ovary, pathologically altered organs, as well as representative specimens of the brain, lung, liver, kidney, spleen, pancreas and intestine, omentum and intra-abdominal lymph nodes, were fixed in 4% PBS buffered paraformaldehyde. They were then evaluated by microscopic analysis of paraffin sections stained with haematoxylin and eosin, and subjected to necessary immunostainings. All early atypical lesions were diagnosed based on their morphology, staining for Ki67 and detection of deleted (floxed-out) *Trp53* and *Rb1* as described earlier[27]. The locations of all lesions were determined by three-dimensional reconstruction of 4-μm-thick serial sections as described previously[39].

Immunohistochemistry and quantitative image analysis. Information regarding all primary antibodies is provided in Supplementary Table 6. Immunohistochemical analysis of paraffin sections of paraformaldehyde-fixed tissue was carried out using a modified ABC technique[37–39]. For immunofluorescence analysis, de-paraffinized or frozen sections and cells were fixed in 4% paraformaldehyde. Ten-minute treatment with 4N HCl and 10 min boiling in 10 mM citric buffer was used to retrieve antigen for detection of BrdU. Staining of theca cells[45] served as a positive internal control for ALDH1 detection. Sections with immunoperoxidase stainings were scanned by ScanScope (Aperio Technologies) with a ×40 objective followed by lossless compression. Sections with immunofluorescent stainings were analysed under an Axioskop 2 (Zeiss) fluorescence microscope equipped with a CCD camera. Quantitative analysis of immunohistochemistry and immunofluorescence experiments were carried out using the ImageJ software (NIH) as described previously[37–39].

Quantitative real-time PCR. All procedures were carried out as described previously[32], with at least three separately prepared RNA samples for each of three independent experiments. A list of the genes tested is included in Supplementary Table 3. The following primers for detection of microRNAs were obtained from Quanta Biosciences: U6 small nuclear RNA (catalogue no. HSRNU6); miR-34a (catalogue no. HSMIR-0034A); miR-34b (catalogue no. MMIR-0034B-5P); miR-34c (catalogue no. HSMIR-0034C-3P); miR-376b (catalogue no. MMIR-0376B).

Statistical analyses. All statistical analyses in this study were carried out using InStat 3.10 and Prism 5.04 software (GraphPad) as described previously[27,37].

31. Corney, D. C., Flesken-Nikitin, A., Godwin, A. K., Wang, W. & Nikitin, A. Y. *MicroRNA-34b* and *microRNA-34c* are targets of p53 and cooperate in control of cell proliferation and adhesion-independent growth. *Cancer Res.* **67,** 8433–8438 (2007).
32. Hwang, C. I. *et al.* Wild-type p53 controls cell motility and invasion by dual regulation of MET expression. *Proc. Natl Acad. Sci. USA* **108,** 14240–14245 (2011).
33. Russo, J. E., Hauguitz, D. & Hilton, J. Inhibition of mouse cytosolic aldehyde dehydrogenase by 4-(diethylamino)benzaldehyde. *Biochem. Pharmacol.* **37,** 1639–1642 (1988).
34. Lawson, D. A., Xin, L., Lukacs, R. U., Cheng, D. & Witte, O. N. Isolation and functional characterization of murine prostate stem cells. *Proc. Natl Acad. Sci. USA* **104,** 181–186 (2007).
35. Xin, L., Lukacs, R. U., Lawson, D. A., Cheng, D. & Witte, O. N. Self-renewal and multilineage differentiation in vitro from murine prostate stem cells. *Stem Cells* **25,** 2760–2769 (2007).
36. Singec, I. *et al.* Defining the actual sensitivity and specificity of the neurosphere assay in stem cell biology. *Nature Methods* **3,** 801–806 (2006).
37. Zhou, Z. *et al.* Synergy of p53 and Rb deficiency in a conditional mouse model for metastatic prostate cancer. *Cancer Res.* **66,** 7889–7898 (2006).
38. Choi, J., Curtis, S. J., Roy, D. M., Flesken-Nikitin, A. & Nikitin, A. Y. Local mesenchymal stem/progenitor cells are a preferential target for initiation of adult soft tissue sarcomas associated with p53 and Rb deficiency. *Am. J. Pathol.* **177,** 2645–2658 (2010).
39. Nikitin, A. Y. & Lee, W. H. Early loss of the retinoblastoma gene is associated with impaired growth inhibitory innervation during melanotroph carcinogenesis in $Rb^{+/-}$ mice. *Genes Dev.* **10,** 1870–1879 (1996).
40. Debacq-Chainiaux, F., Erusalimsky, J. D., Campisi, J. & Toussaint, O. Protocols to detect senescence-associated beta-galactosidase (SA-βgal) activity, a biomarker of senescent cells in culture and *in vivo*. *Nature Protocols* **4,** 1798–1806 (2009).
41. Matoso, A., Zhou, Z., Hayama, R., Flesken-Nikitin, A. & Nikitin, A. Y. Cell lineage-specific interactions between Men1 and Rb in neuroendocrine neoplasia. *Carcinogenesis* **29,** 620–628 (2008).
42. Zhou, Z., Flesken-Nikitin, A. & Nikitin, A. Y. Prostate cancer associated with p53 and Rb deficiency arises from the stem/progenitor cell-enriched proximal region of prostatic ducts. *Cancer Res.* **67,** 5683–5690 (2007).
43. Zhou, Z. *et al.* Suppression of melanotroph carcinogenesis leads to accelerated progression of pituitary anterior lobe tumors and medullary thyroid carcinomas in $Rb^{+/-}$ mice. *Cancer Res.* **65,** 787–796 (2005).
44. Rugh, R. In *The Mouse: Its Reproduction and Development* 7–43 (Oxford Univ. Press, 1990).
45. Vermot, J., Fraulob, V., Dolle, P. & Niederreither, K. Expression of enzymes synthesizing (aldehyde dehydrogenase 1 and reinaldehyde dehydrogenase 2) and metabolizaing (Cyp26) retinoic acid in the mouse female reproductive system. *Endocrinology* **141,** 3638–3645 (2000).

©2013 Macmillan Publishers Limited. All rights reserved